THESIS

DYNAMICS OF H3 AND H2B OCTAMER VARIANTS

Submitted by

Abigail Lea McVay

Department of Biochemistry and Molecular Biology

In partial fulfillment of the requirements

For the Degree of Master of Science

Colorado State University

Fort Collins, Colorado

Spring 2020

Master's Committee:

Advisor: Jeffrey C. Hansen

Sandra Quackenbush
Jennifer DeLuca

ABSTRACT

DYNAMICS OF H3 AND H2B OCTAMER VARIANTS

Introductions of alterations within a nucleosome can lead to drastic changes to the accessibility and stability of genetic material during various phases of the cell cycle. To understand these changes, three octamer mutants were recombined, reconstituted with a high affinity tandem repeat sequence, and tested using a combination of *in vitro* experimental methods. All Tailless, H2BTL and an H2BTL & H3TL nucleosomal array mutants were sedimented, digested, re-associated, and visualized in order to determine the role of histone tails and their influence on chromatin condensate structure. The All Tailless octamer mutant expressed an inability to form complex molecular structures, suggesting that histone tails are necessary to further the process of chromatin condensate association and subsequent folding. The H2BTL mutant expressed high levels of concentration and an increased level of association compared to the other mutants. This lead to the assumption that the exclusion of only one histone tail lead to a greater ability to associate compared to mutants lacking two or more tails. The H2BTL & H3TL mutant had a possibility of two distinct populations within solution, suggesting that the exclusion of at least two tails led to a loosely compacted and easily accessible chromatin condensate structure. In summary, this data suggests that as histone tails are excluded from octamer mutants, the chromatin condensates expresses a decreased ability to form higher degrees of compaction. Exclusion of histone tails from octamer mutants also resulted in a more accessible 601-12 tandem repeat sequence susceptible to various changes.

ACKNOWLEDGMENTS

Thank you to Dr. Jeffrey Hansen for being my advisor and allowing me to gain such meaningful experiences in his lab during my undergraduate and graduate time at CSU. Also for being one of my committee members.

Thank you to Jennifer Deluca and Sandra Quackenbush for being on my Masters committee and supporting me as I completed my experiences at CSU.

Thank you to all of the individuals involved within the department of Biochemistry and Molecular Biology at CSU for being engaging and supportive.

Thank you to Dr. Hataichanok Scherman, Dr. Laurie Stargell, Dr. Olve Peerson, Dr. Tom Santangelo, and other department faculty for providing the Hansen lab members with some of the space, materials, and equipment necessary for completing our experiments.

Thank you to everyone in the CSU College of Veterinary Medicine and Biomedical Sciences Dean's Office for helping me to further develop my management, writing, and communicative skills.

Thank you to Dr. Farida Safadi-Chamberlain, Dr. Eric Ross, Dr. LUBNA Tahtamouni, Dr. Tom Santangelo, and Dr. Paul Laybourn for allowing me to gain experiences teaching other students in lab and in lecture settings.

Thank you to Eric Seidel, CJ McDonald, and the other previous graduate students within Dr. Hansen's lab for providing protocols and advice.

Thank you to Mark Conolly for helping me with my understanding of the analytical ultracentrifuge and various protocols.

Thank you to Tommy Tolsma, the Post Doc in the lab for giving me advice and supporting me. Also for helping me with the microscope and other pieces of equipment within the lab.

Thank you to Amanda Kuerzi and Vimalkannan Kaliraj for letting me bounce off ideas and sharing various articles as I completed my experiments.

Thank you to Matthew Funk for helping me with various experiments and for challenging me on how to think and explain processes.

Thank you to all of the other undergraduates in Dr. Hansen's lab for helping me with various experiments and for making time in the lab so meaningful.

TABLE OF CONTENTS

LIST OF FIGURES

INTRODUCTION

Understanding the dynamics of nucleosomes and the potential variations within an octamer is essential in understanding how modifications to the core histones may affect the level of DNA compaction and accessibility. Modifications to the accessibility of DNA and subsequent compaction often have a significant impact many cellular processes such as gene expression, DNA replication, transcription, translation, and post-translational modifications[18].

Nucleosomal Arrays

A canonical nucleosome is composed of a roughly 147 base pair sequence of DNA wrapped around a protein octamer that contains two copies of each of the core histones H2A, H2B, H3 and H4[8]. Formation of this nucleosome occurs in sequential steps. First, both copies of histones H3 and H4 interact to form a tetrameric structure. It is thought that the N-terminal tail of the H4 histone and its interaction with the N-terminal region of histone H3 has a significant role in regulating the overall folding of DNA within a nucleosome[1]. Following formation of the H3-H4 tetramer and its interaction with DNA, heterodimers of H2A and H2B interact to form the Nucleosome Core Particle[29]. Histone-DNA interactions within the nucleosome are stabilized with the presence of lysine and arginine residues within the N-terminal histone tails[18]. Further organization of these nucleosomes, upon exposure to increasing magnesium concentrations, leads to the formation of a nucleosomal array in 10-nm confirmation that is further packaged into a chromatin structure with the addition of an H-linker histone[8]. Nucleosome positioning and accessibility along DNA is influenced by a multitude of factors including temperature, salt concentrations, cell cycle stages, pH of the solution, and histone

variations within an octamer[1]. Nucleosomal accessibility can be determined using arrays consisting of a high affinity 601 tandem repeat DNA sequence and octamer mutants[17].

Octamer Variations

Through studying the dynamics and structural changes of octamer variations or mutants, and their impacts on nucleosomal positioning, compaction of chromatin and it effect on complex cellular processes can be better understood. Variations within an octamer can drastically impact the structure and stability of chromatin condensates. Incorporation of some histone mutants could also have a greater impact on this stability than others. For example, an H4 tailless mutant could lead to changes in an octamers ability to slide across a sequence of DNA during certain phases of the cell cycle. An H2A tailless mutant has also been shown to significantly increase an octamers mobility and thus cause a decrease in nucleosome stability[1]. Changes in the stability of the nucleosome would impact the favorability for nucleosomal arrays to form more complex chromatin condensates, and could thus have a detrimental effect on essential cellular functions[1].

Experimental Procedures and Hypothesis

To determine the effects of histone H3 and histone H2B on chromatin stability and packaging, three octamer mutants were tested. The tested recombinant octamer mutants were as follows: an octamer containing all tailless histones ("All Tailless"), an octamer with a tail removed from only H2B ("H2BTL"), and an octamer containing histones excluding tails on the H2B and H3 histones ("H2BTL & H3TL"). These recombinant Xenopus octamer mutants were reconstituted with a 601-12 DNA sequence and the resulting arrays were later analyzed via several experimental methods[7,22]. The 601-12 tandem repeat DNA sequence was adapted from a 1998 protocol in which optimal octamer positioning and high binding affinity was determined[17]. Reconstituted arrays were sequentially digested with an EcoRI or EcoRV enzyme and spun in an

analytical ultracentrifuge to determine levels of octamer to DNA saturation and concentration[5,16]. After desired saturation levels were obtained, Magnesium 50 curves were utilized to determine the ability of self-association[2]. Further confirmation of nucleosome saturation and accessibility along the 601-12 tandem repeat sequence was confirmed with the use of a Micrococcal Nuclease digestion. Accessibility and exchange between chromatin condensates was then tested with fluorescence microscopy. It is hypothesized that as histone tails are withheld from octamers, the overall stability of the array would decrease, whereas an increase in accessibility within the arrays and resulting chromatin condensate structures may be determined.

METHODS

Octamer Preparation

Respective Xenopus histone proteins - H2A, H3, H4, and H2B - were obtained from glycerol stocks of c-HP. The histones were then dialyzed against 1 M NaCl (10 mM tris-Cl pH 7.5, 1 mM EDTA, 5 mM ß-mercaptoethanol), concentrated to about 10 mg/ml, and resuspended in 8 M unfolding buffer (6 M guanidinium HCl, 1 M tris pH 7.5, 5 mM DTT). Each histone was dissolved in this unfolding buffer for at least 1 hour. Concentrations of the unfolded histone proteins were calculated by measuring the OD_{276}. Using the respective OD_{276} values for absorbance, extinction coefficients, molecular weight, the molarity of each histone was calculated. The total number of µmoles was then calculated using this molarity and the remaining volume of each histone. The total volume of each histone necessary to obtain optimal octamer formation was calculated by dividing the "µmoles per reaction" by the total µmoles and then by the volumes of each histone. A 10% increase of histones H2A and H2B was also accounted for. The total amount of milligrams of each histone to be added into the octamer reconstitution was then calculated. A final concentration of 1 mg/mL solution containing all four histones was obtained.

After calculating the necessary milligrams of each histone, the respective histones were placed in a dialysis bag containing an appropriate volume of refolding buffer (2 M NaCl, 1 M tris pH 7.5, 0.5 M EDTA, 5 mM ß -mercaptoethanol) and dialyzed against the same refolding buffer at 4°C, changing the buffer solution twice within a minimum of 18 hours. Following dialysis, the octamer solution was transferred from the dialysis bag and spun at 3,000 rpm to remove any precipitate. The octamer solution was then concentrated in an ultra-centrifugal filter device down to roughly 500 µL. The concentrated sample was washed from the filter using 500 µL of

refolding buffer. The sample was again spun at 3000 rpm to remove any precipitate, then injected into the superdex 200 FPLC column that had been previously equilibrated with refolding buffer. The sample was run for a full column volume (about 120 mL) at 1 mL/min. The respective octamer was collected in fraction tubes after running roughly 60 to 70 mL through the column. Fractions containing dimer and aggregate were discarded. Confirmation of octamer presence was done by running samples of each fraction tube on an sodium dodecyl sulfate (SDS) gel. The respective fraction tubes containing only the desired octamer were pooled and the sample was concentrated again using an ultra-centrifugation filter device. The octamer was then washed from the device and placed in an eppendorf tube with a desired concentration less than 15 mg/mL.

601-12 Insert Preparation

A pre-culture of 601-12 plasmid containing DH5α bacteria in LB (7 g NaCl, 7 g tryptone, 3.5 g yeast extract, and MilliQ H_2O) and ampicillin was incubated overnight. Six flasks, each containing TB (16.8 g yeast extract, 8.4 g tryptone, 2.8 mL glycerol, 70 mL KH_2PO_4/K_2PO_4, and MilliQ H_2O) were prepared for the next day. After roughly 24 hours, the 601-12 pre-culture was distributed into each of the six LB flasks in addition to respective volumes of ampicillin. Cultures were grown overnight in 37°C shaker for 18-22 hours, then harvested at 4000 rpm for 15 min. The resulting pellets were resuspended in lysis buffer. NaOH-SDS was added and the solution was incubated on ice for 20 minutes. Cold K/Acetate was added and the solution was mixed and incubated on ice for an additional 30 minutes. The solution was then spun at 8000 rpm for 30 minutes at 4°C then filtered to remove any precipitate. 0.55 volumes of Isopropanol was added to the solution and left at room temperature for 15 minutes before spinning the solution again at 8000 rpm for 45 minutes at 20˚C. The resulting pellets were stored at room

temperature overnight to allow for complete evaporation of the isopropanol. The resulting pellets were resuspended in TE (10 mM tris pH 8.0, 50 mM Na_2/EDTA, and MilliQ H_2O) and incubated with a respective volume of RNase A overnight. 40% PEG 6000 and 5M NaCl was added and the solution was incubated on ice for 30 minutes then spun at 5000 rpm for 20 minutes at 4˚C. The pellet was again resuspended in TE. RNA digestion and separation was confirmed with a test digest. An equal volume of 25:24:1 phenol: chloroform: isoamyl alcohol was added and the suspension was vortexed, then spun at 12,000 rpm for 10 minutes at 20°C. This process was repeated until no white interphase residue remained. Isopropanol and 3M NaAc was added and the solution was stored in the freezer for at least overnight. The solution was spun at 13100 rpm for 20 minutes at 4°C. The pellet was then washed with an equal volume of cold 0.75 EtOH and spun again at 13100 rpm for 20 minutes at 4˚C. The pellets were left at room temperature overnight to evaporate any remaining ethanol and resuspended in TE. A test digest was performed and visualized on a 1% agarose gel to confirm the presence of our desired insert. A bulk digest was then performed for a minimum of 24 hours and visualized on a 1% agarose gel. The digested sample, with the addition of glycerol, was then run close to a rate of 1 mL/min through a sephacryl S-1000 column equilibrated with TEN buffer (10 mM tris pH 7.8, 1 mM EDTA, 50 mM NaCl, and MilliQ H_2O). Fractions were tested on a 1% agarose gel to determine the presence of the desired 601-12 insert. Fractions containing only the insert (about 2500 bp) were pooled in a solution containing Isopropanol and NaAc then stored in the freezer for at least overnight. The solution was spun at 13100 rpm for one hour at 4°C, washed again with cold 0.75 EtOH and spun at 13100 rpm for an additional hour at 4˚C. The pellet was then stored at room temperature overnight to allow for ethanol evaporation, then again resuspended in about 1 mL of

TE. The concentration was determined using a 1:10 dilution against TE. To verify presence of insert, the sample was run again on a 1% agarose gel.

601-12 Insert and Octamer Reconstitution

Using the respective molecular weight and concentration values for the 601-12 plasmid insert, The DNA molar concentration was calculated and expressed in Moles/L. The necessary volume of 601-12 insert to be added was then calculated by dividing 200 µgrams by the DNA concentration. The amount of octamer necessary for optimal reconstitution was calculated by obtaining the respective molecular weight and concentration. Optimal ratios of octamer were determined. The desired amounts of 601-12 insert and octamer were added to a respective volume of 2 mM NaCl (5 M NaCl, 1 M Tris pH 7.8, 0.5 M EDTA, and MilliQ H_2O) to bring the final volume of the reconstitution sample to 666.67 µL. The samples were then placed in a dialysis bag and dialyzed in a series of four cold 1 L buffers for a minimum of four hours per buffer: 1 M NaCl (NaCl, 1 M tris pH 7.8, 0.5 M EDTA, 1 M DTT, and MilliQ H_2O), 0.75 M NaCl (NaCl, 1 M tris pH 7.8, 0.5 M EDTA, 1 M DTT, and MQH_2O), 2.5 mM NaCl (NaCl, 1 M tris pH 7.8, 0.5 M EDTA, 1 M DTT, and MilliQ H_2O), and 2.0 mM NaCl (NaCl, 1 M tris pH 7.8, 0.5 M EDTA, 0.2 M PMSF, and MilliQ H_2O). Following dialysis, the sample was removed from the dialysis tubing and placed in an eppendorf tube. Confirmation of reconstitution was performed using an EcoRI or EcoRV digestion and run on a 1% agarose gel. Saturation levels were estimated and confirmed using Analytical Ultracentrifugation. The resulting arrays were saved in 1.5 mL eppendorf tubes in the fridge for future use. Desired saturation levels were roughly 1 histone per 601 repeat (12 histones along a single 601-12 insert).

Analytical Ultracentrifugation

In order to determine sedimentation coefficients of the reconstituted arrays, analytical ultracentrifugation (AUC) was performed. Samples to be analyzed via analytical ultracentrifugation were created by diluting the reconstituted arrays in a new Eppendorf tube with buffer 4: 2 mM NaCl (NaCl, 1 M tris pH 7.8, 0.5 M EDTA, 0.2 M PMSF, and MQH_2O) up to 400 µL. The AUC samples were then placed one of the sectors of a two sector AUC cell housing unit. The remaining sector was then filled with buffer 4 to serve as a reference. The cell housing unit was then sealed with fill hole gaskets and placed in the ultracentrifuge and run for roughly an hour. The resulting sedimentation coefficient values (S-values) given by the G(s) distributions were then used to determine levels of octamer saturation along the 601-12 DNA insert. If needed, the reconstituted were again with the addition of respective amounts of DNA and octamer and reanalyzed with AUC runs until a desired level of saturation was achieved.

EcoRI/EcoRV Digestion

Following analytical ultracentrifugation, a mononucleosome digest was performed. 5 µL of arrays, 4 µL of CutSmart buffer, 1 µL of EcoRI or EcoRV, and 30 µL of MilliQ H_2O were combined in an eppendorf tube and placed in the hot water bath for at least one hour. Using a 1% agarose gel, half of the digested array was run with 4 µL of 6X loading dye and the remaining half was run with 4 µL of a 25% glycerol/EDTA solution.

Magnesium 50 Curves

The level of array self-association was determined using Magnesium 50 curves. In a series of eppendorf tubes, a small amount of array was added to a $MgCl_2$ concentration of 50 mM, and of buffer 4: 2 mM NaCl (NaCl, 1 M Tris pH 7.8, 0.5 M EDTA, 0.2 M PMSF, and MilliQ H_2O) to make varied concentrations of magnesium 50 assays: 0 mM, 1 mM, 2 mM, 2.5 mM, 3 mM, 3.5

mM, 4 mM, 5 mM, and 6 mM, 8 mM, and 10 mM respectively. Solutions were kept at room temperature for at least 20 minutes, then placed in a centrifuge at 20,000 g for 15 minutes. The supernatant was then collected without disturbing the pellets. The OD_{260} was measured for each of the supernatants and a scatter plot was generated.

Micrococcal Nuclease

Micrococcal Nuclease (MNase) experiments were performed in order to determine the accessibility of DNA within the arrays. Based on the array concentration, a set of time points and the amount of array, reaction buffer, Micrococcal Nuclease enzyme, and stop reaction buffer was determined. For the purposes of this experiment, time points were chosen as follows: 0 minutes, 5 minutes, 10 minutes, and 15 minutes. Reaction buffers were made containing $MgCl_2$, $CaCl_2$, buffer 4 (with no EDTA or PMSF), and a calculated volume of array. After a 15 minute incubation, Micrococcal Nuclease enzyme was added. Immediately following addition of Micrococcal Nuclease, the appropriate amount of the reaction containing the array was removed and placed in respective eppendorf tubes containing an equal volume of stop reaction buffer (EGTA, EDTA, buffer 4 (no EDTA and PMSF), and SDS-loading dye). Each time point sample was then run on a 1% agarose gel to determine the level of accessibility within the array.

Fluorescence Microscopy

The point at which arrays were fully associated was determined using the magnesium 50 curves. Accounting for a little extra magnesium to ensure total association, SYBR® Gold buffers were created to obtain a magnesium concentration of 20 mM. Buffers were made at 1x, 0.01x and 0x of SYBR® Gold with buffer 4 (0.25 mM EDTA and NO PMSF). Samples were prepared by adding 5 μL of array to buffer 4 (0.25 mM EDTA and NO PMSF) up to a total volume of 2 mL. These samples were stored at room temperature for roughly 20 minutes before adding them to

labeled poly-l-lysine coated dishes. The dishes were then spun at 3,000 rpm for about 3 minutes. Excess liquid was removed, leaving some on the cover slip. 2 mL of the 1x buffer was then added and the dishes were stored at room temperature for about one minute. The 1x buffer was removed and 2 mL of the 0x buffer was added. After another minute this wash step was repeated with the 0x buffer. The liquid was removed and 2 mL of the 0.01x buffer was added to allow for imaging of the arrays. Images of the arrays were gathered using a confocal microscope with an excitation wavelength of 488 nm. Subsequent analysis was performed using SlideBook and ImageJ software.

RESULTS

Octamer Preparation

All Tailless

Fast Protein Liquid Chromatography (FPLC) of the "All Tailless" octamer mutant registered a minimal peak around 42 mL, a large peak around 68 mL, and a peak around 81 mL (Figure 1a). Collection tubes containing volumes from each peak were collected and run on an SDS-gel. Only tubes 10 – 20 corresponded to the mAU peak around 68 mL and were determined to contain the "All Tailless" octamer mutant. These tubes were pooled and concentrated for later use. The resulting "All Tailless" octamer mutant had a final concentration of 4.88 mg/mL.

H2BTL

UV readings of the "H2BTL" octamer mutant registered a mAU peak around 40 mL, a peak around 60 mL, and a peak around 80 mL. There was also a peak registered around 115 mL (Figure 1b). It was also noted that the peaks around 40 mL, 60 mL, and 80 mL had a higher mAU value for the UV reading compared the corresponding peaks in the "All Tailless" and "H2BTL and H3TL" octamer mutants. Collection tubes 9 – 17 were determined to contain the expected "H2BTL" octamer mutant. These tubes corresponding to the mAU peak registered around 60 mL were pooled and concentrated for later use. The resulting "H2BTL" octamer mutant had a final concentration of 9.092 mg/mL.

H2BTL & H3TL

The FPLC UV readings for the "H2BTL & H3TL" octamer mutant registered a potential peak around 43 mL, a peak around 64 mL, and a peak around 80 mL (Figure 1c). Only tubes 4 – 14 corresponding to the mAU peak registered around 64 mL and containing the expected "H2BTL

& H3TL" octamer mutant were pooled and concentrated for later use. The resulting "H2BTL & H3TL" octamer mutant had a final concentration of 6.909 mg/mL.

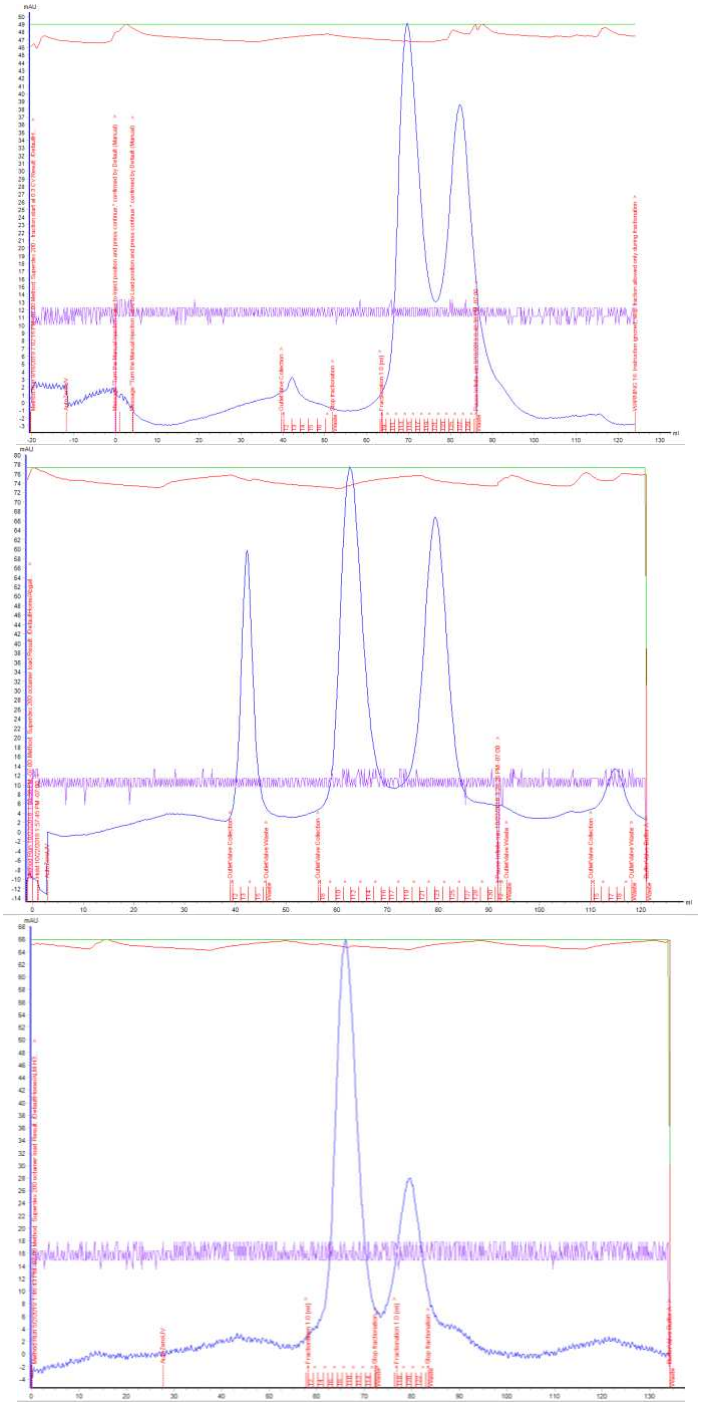

Figure 1. From left to right, UV readings of aggregate, octamer, and dimer mAU peaks are recorded. a) Graph depicts the "All Tailless" mutant octamer with a minimal aggregate peak. b) Graph depicts the "H2BTL" mutant octamer with high aggregate and dimer peaks, as well as an additional peak thought to be monomer. c) Graph depicts the "H2BTL & H3TL" mutant octamer with minimal aggregate present.

601-12 Insert Preparation

After isolation of the desired plasmid and resuspension, digestions were performed. Digestions were performed on samples collected before and after the addition of RNase A, of the PEG supernatant, and of the resuspended pellet. The expected five bands were visualized within the resuspended pellet sample. Sequential steps of the 601-12 insert preparation were tested with digestions and again visualized on agarose gels. After removal of the white interphase residue, another digest was performed and the expected bands were visualized. Prior to running the resuspended sample through a sephacryl S-1000 size exclusion column, a bulk digest was performed and run on an agarose gel. The expected bands were again visualized. Running the sample through a size exclusion column yielded a single desired band insert at roughly 2500 base pairs. The 601-12 tandem repeat sequence had a final concentration of 1.3705 mg/mL. This 601-12 insert was later reconstituted with the desired octamer mutants.

601-12 Insert and Octamer Reconstitution

Each octamer mutant was combined with appropriate volumes of buffer 4 (No EDTA or PMSF) and of the 601-12 tandem repeat insert. Ratios of octamer to 601-12 insert were originally added between R-values of 0.8 and 1.0. Samples were dialyzed in refolding buffer (containing an adjusted EDTA ratio and no ß-Me) and four additional buffers that decreased in NaCl concentration. The mutants were dialyzed in each for a minimum of four hours. Success of each reconstitution was determined via analytical ultracentrifugation and EcoRI or EcoRV digests. If G(s) distributions recorded lower or higher sedimentation coefficients than desired, arrays were readjusted with appropriate volumes of 601-12 insert or of the octamer mutants and again dialyzed with the respective buffers.

Analytical Ultracentrifugation (AUC)

All Tailless

The G(s) distribution resulting from analytical ultracentrifugation of the All Tailless array recorded a sedimentation coefficient (S-value) just above 24 S at a boundary fraction of 50. Analytical centrifugation of this array recorded the expected s-curve and no other populations were expected to be present (Figure 2a).

H2BTL

Analytical Ultracentrifugation of the H2BTL mutant array resulted in a G(s) distribution with a recorded S-value just above 28 S at a boundary fraction of 50. The G(s) distribution for the H2BTL sample also recorded the expected curve, suggesting that only the desired population was present (Figure 2b).

H2BTL & H3TL

The sedimentation coefficient for the "H2BTL & H3TL" mutant array was recorded around 37 S at a boundary fraction of 50 was found to be 37 S. The G(s) distribution for this array also suggested the presence of a potential second population around 49 S (Figure 2c). Ratios of 601-12 tandem insert to the H2BTL & H3TL mutant octamer were readjusted and the array sample was again dialyzed before moving to the EcoRI or EcoRV digestion.

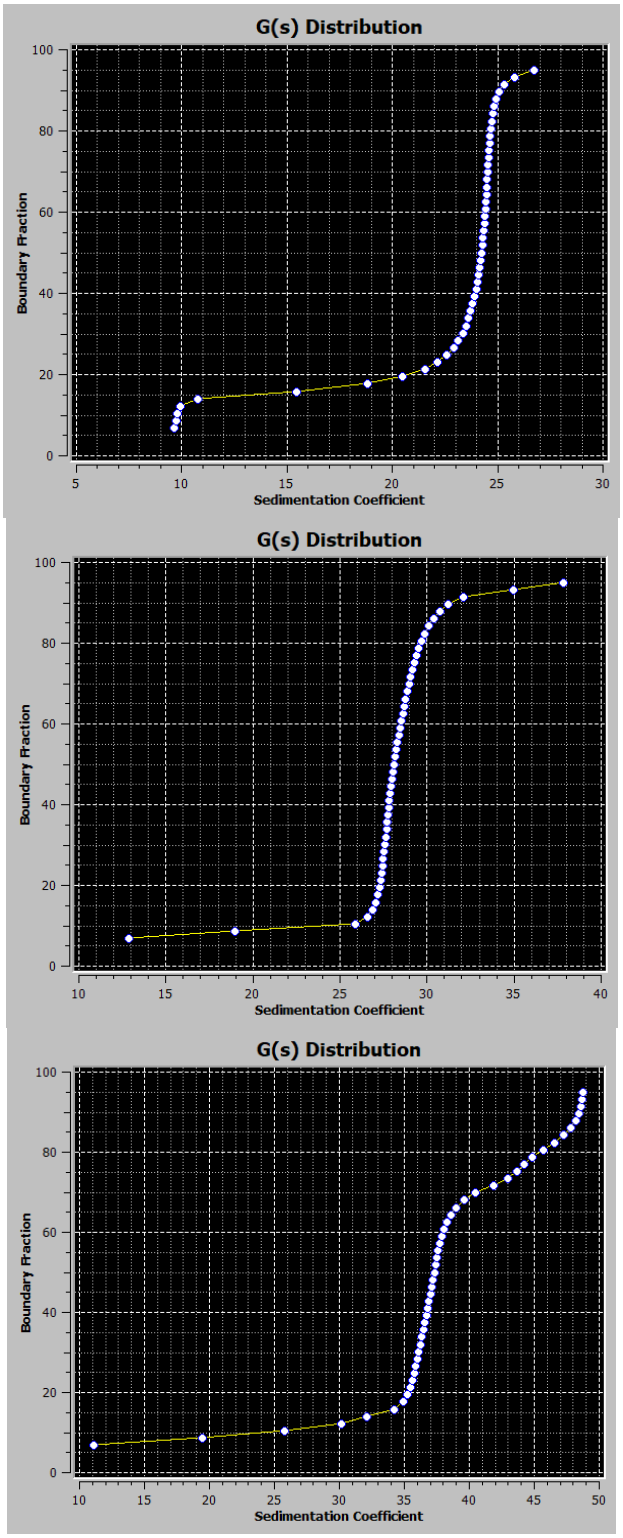

Figure 2. a) Reflects the AUC sedimentation coefficients for the "All Tailless" mutant array with an S-value of 24 at a boundary fraction of 50. b) Reflects the AUC sedimentation coefficients for the "H2BTL" mutant array with an S-value of 28 at a boundary fraction of 50. c) Reflects the AUC sedimentation coefficients for the "H2BTL & H3TL" mutant array with an S-value of 37 at a boundary fraction of 50 and potential second population around 49 S.

EcoRI/EcoRV Digestion

All Tailless

The All Tailless mutant array depicted a smearing pattern when run on an agarose gel in all respective lanes. Separate band sizes were largely indistinguishable in each lane. No presence of "free" 601-12 insert was detected near the bottom of the lanes containing the All Tailless mutant array and loading dye. This All Tailless mutant array samples was later tested for ability of association into higher order structures with magnesium 50 curves.

H2BTL

The H2BTL mutant array depicted a smearing pattern when run on a gel in all appropriate lanes. This array was also digested with EcoRV as a comparison. No distinct feature differences were detected with the use of EcoRI and EcoRV. The gel was difficult to visualize, but separate band sizes were also largely indistinguishable using both enzymes. No presence of "free" 601-12 insert was detected. The ability for this mutant array to associate into higher order chromatin condensates was also tested for the H2BTL mutant array using magnesium 50 curves.

H2BTL & H3TL

The "H2BTL & H3TL" mutant array, run on the same gel as the H2BTL mutant array, also depicted a similar smearing pattern in each lane. Like the H2BTL mutant array, the H2BTL & H3TL mutant array was digested with EcoRI and with EcoRV as a comparison. No distinct feature differences were detected with the use of EcoRI and EcoRV for this mutant array. Separate band sizes were again largely indistinguishable in lanes containing the H2BTL & H3TL mutant array with either restriction enzyme. Although the gel was difficult to visualize, No presence of "free" 601-12 insert was detected in the lanes containing the mutant array and loading dye. Magnesium 50 curves were also completed using this mutant array.

Magnesium 50 Curves

All Tailless

Three trials were performed for the All Tailless mutant array. The absorbance (A_{260}) values for the All Tailless mutant array remained at or around 0.3, normalized to 0.9, in all trials of the Mg50 curves. This mutant array did not express a significant decrease in values and did not reach 50% association or an absorbance below 0.1 (Figure 3a). Due to absorbance values reflecting no further association in increasing $MgCl_2$ concentrations, the All Tailless mutant arrays were not utilized for the Micrococcal Nuclease or fluorescence microscopy experiments.

H2BTL

Three trials were performed for the H2BTL mutant array. The absorbance values were averaged and normalized. The absorbance (A_{260}) values for the H2BTL mutant array recorded a steady decrease as the $MgCl_2$ concentration was increased in the solution. The absorbance values for this array were recorded at 50% of the highest absorbance reading when centrifuged in a solution of 5 mM $MgCl_2$. Absorbance values around zero were recorded for H2BTL mutant arrays centrifuged in solutions around 8 mM $MgCl_2$ (Figure 3b).

H2BTL & H3TL

Similar to the other mutant arrays tested, three trials were performed for the H2BTL & H3TL mutant array. The absorbance values were averaged and normalized. The absorbance (A_{260}) values for the H2BTL & H3TL array recorded a similar decrease when compared the H2BTL array mutant as the $MgCl_2$ concentration increased. The H2BTL & H3TL mutant array recorded absorbance values at 50% associated the highest value when centrifuged with solutions containing 6 to 7 mM $MgCl_2$. These mutant arrays were expected to record absorbance values around zero when centrifuged with $MgCl_2$ solutions closer to 10 mM to 12 mM (Figure 3c).

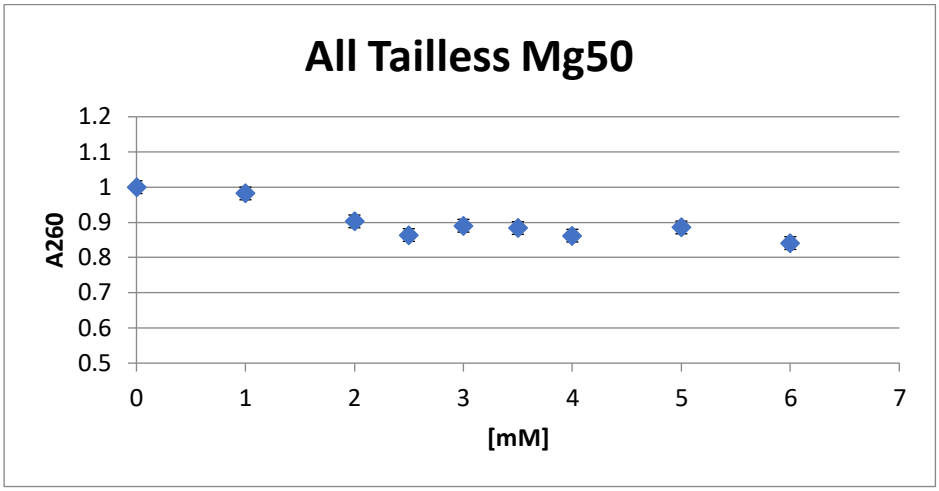

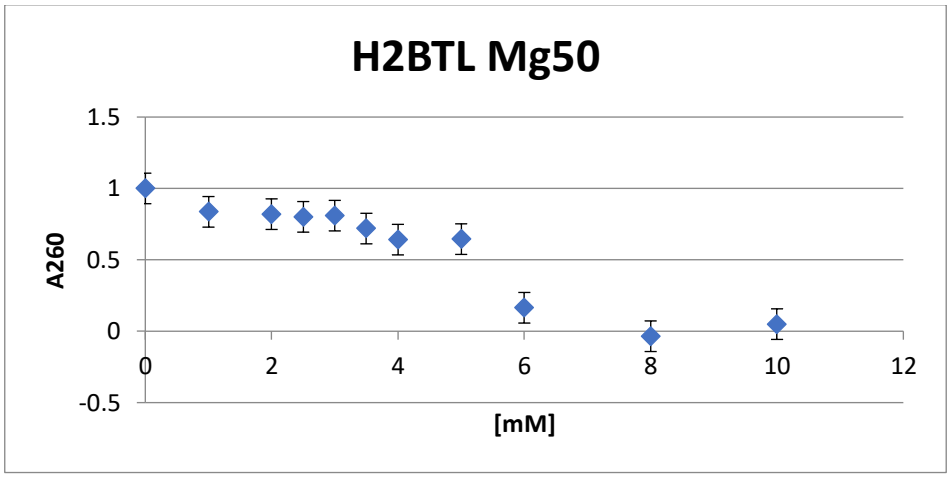

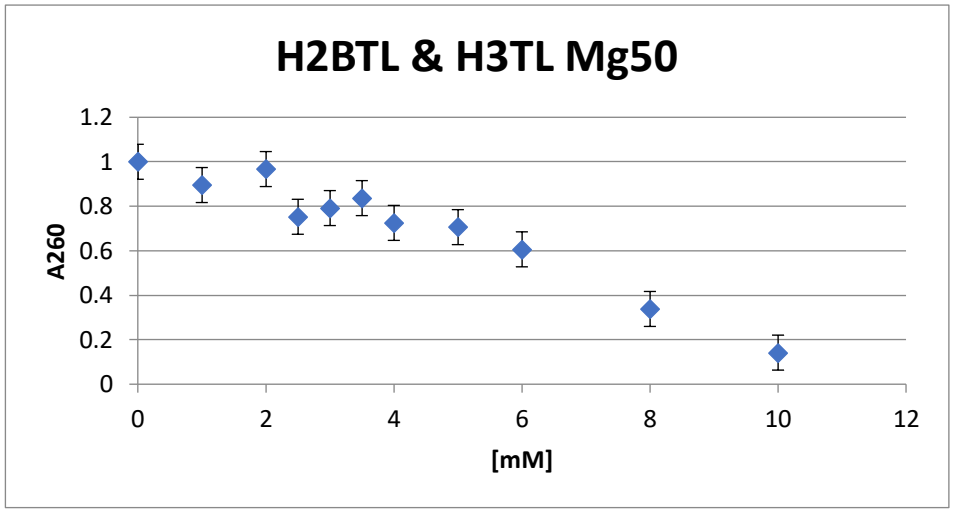

Figure 3. a) Depicts the Mg50 Curve for the "All Tailless" mutant array. b) Depicts the Mg50 Curve for the "H2BTL" mutant array. c) Depicts the Mg50 Curve for the "H2BTL & H3TL" mutant array.

Micrococcal Nuclease Digestion

H2BTL

Immediately following addition of the diluted Micrococcal Nuclease (MNase) enzyme, about 4.44 μL of the reaction solution was removed and placed in the zero minute time point tube containing the stop reaction buffer. This tube reflected minimal to no digestion. After five minutes, the solution was partially digested and began reflecting a ladder pattern with distinct band sizes on the agarose gel. The 10 and 15 minutes points reflected further levels of digestion along the 601-12 insert within the H2BTL mutant array. After the 15 minute time point, the H2BTL sample was not fully digested and two band sizes remained (Figure 4a). Complete digestion was expected to occur at later time points.

H2BTL & H3TL

The H2BTL & H3TL array sample reflected similar results to the H2BTL array. At the zero minute time point, no digestion activity was detected. After five minutes, MNase reaction reflected initial levels of digestion and began reflecting a distinct band sizes in a ladder pattern on the agarose gel. The 10 and 15 minute time points also reflected further progress of digestion similar to the H2BTL mutant array. After the 15 minute time point, two distinct band sizes were visible on the agarose gel (Figure 4b). Complete digestion was expected to occur for this mutant array at later time points.

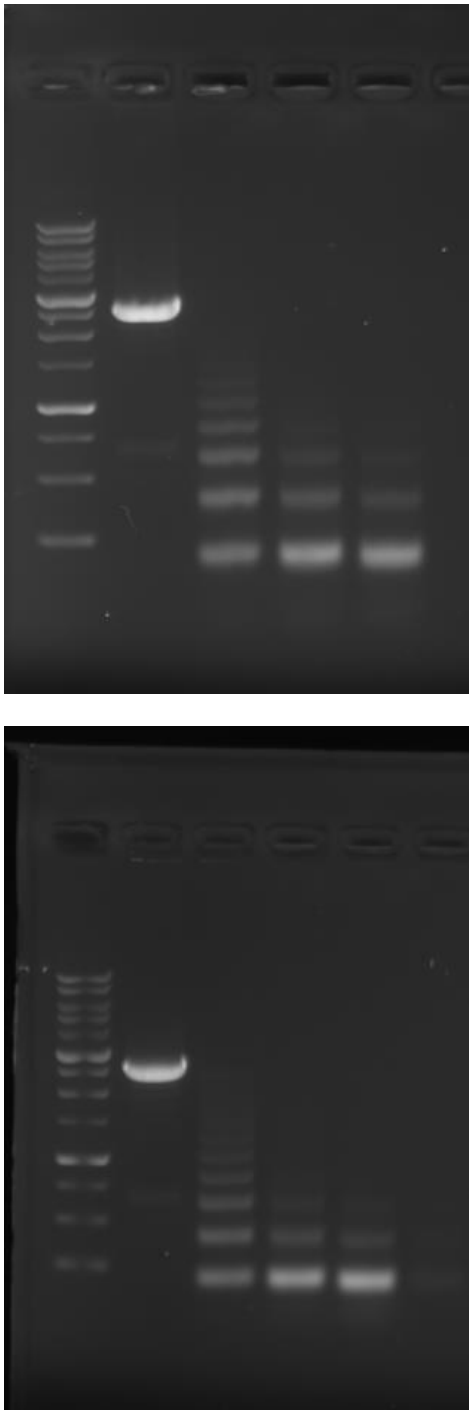

Figure 4. a) Depicts an MNase digestion of the "H2BTL" mutant array at the following time points: 0 minutes (lane 2), 5 minutes (lane 3), 10 minutes (lane 4), and 15 minutes (lane 5). b) Depicts an MNase digestion of the "H2BTL & H3TL" mutant array at the following time points: 0 minutes (lane 2), 5 minutes (lane 3), 10 minutes (lane 4), and 15 minutes (lane 5). Both gels contained the 1 Kb ladder in lane 1 on the left.

Fluorescence Microscopy

"Wild-type"

"Wild type" arrays with non-mutant histones were used as a control for the fluorescence microscopy experiments. Five images were taken of a dish containing this array. Each image contained a high number of chromatin condensates on the coverslip with average condensate diameters in each of the 5 images as follows: 0.215 μm, 0.214 μm, 0.237 μm, 0.210 μm, and 0.206 μm (Figure 5a). Between 600 and 700 chromatin condensates were found in each image plane.

H2BTL

Five images were also taken of the dish containing H2BTL mutant array. Each image reflected less condensates present on the coverslip and average condensate diameters in each of the five images as follows: 0.355 μm, 0.385 μm, 0.354 μm, 0.271 μm, and 0.306 μm (Figure 5b). Each image for the H2BTL mutant array had between 340 to 430 chromatin condensates in the viewable plane.

H2BTL & H3TL

Five images were again taken of a dish containing the H2BTL & H3TL mutant array. Each image reflected a significant decrease in the amount of chromatin condensates present and average condensate diameters in each image as follows: 0.783 μm, 0.699 μm, 0.698 μm, 0.0.691 μm, and 0.689 μm (Figure 5c). The dish for the H2BTL & H3TL array had between 150 to 210 condensates within viewable plane.

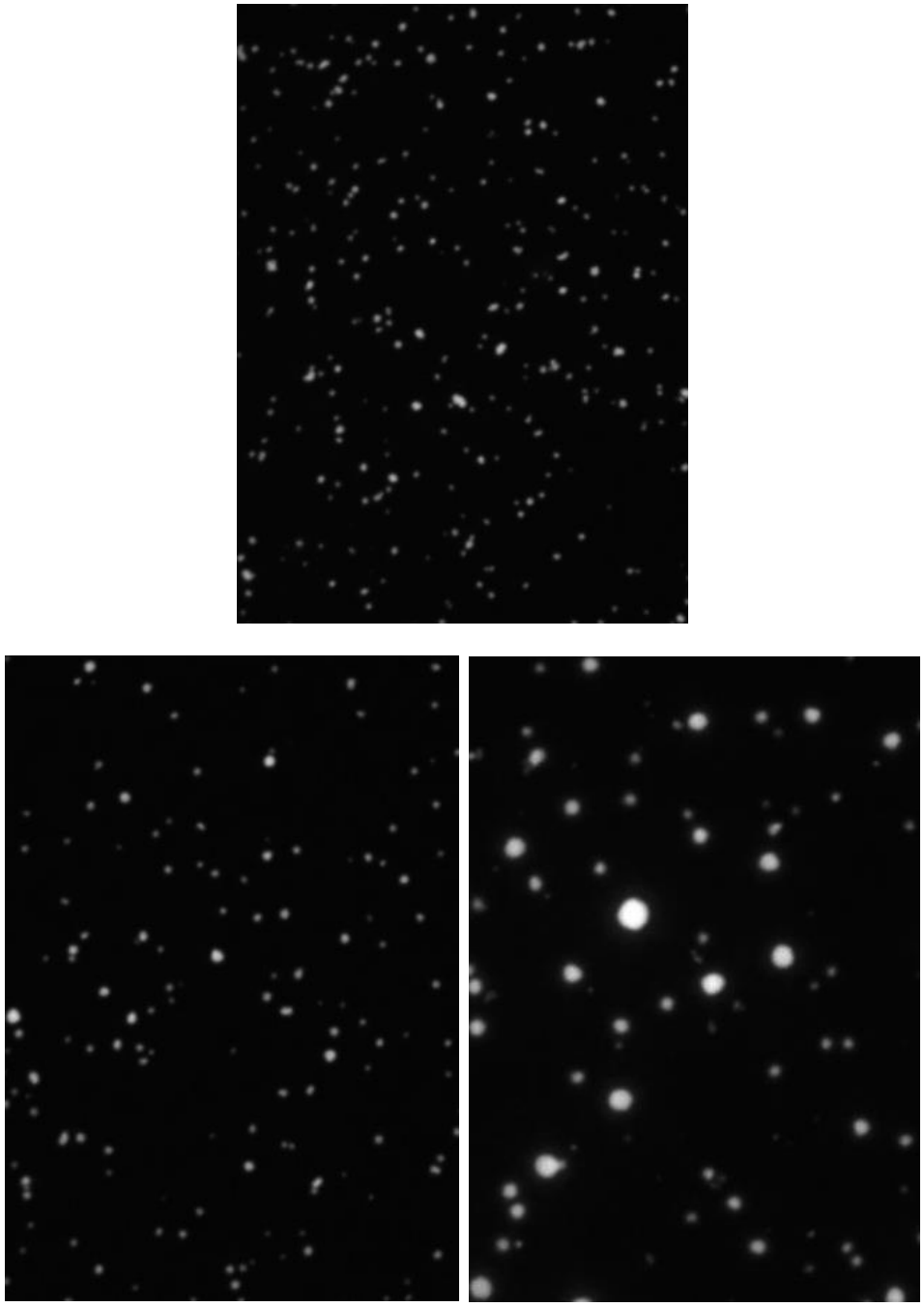

Figure 5. a) Depicts a Confocal microscope image of a “wild-type” array sample stained with SYBR® Gold. b) Depicts a Confocal microscope image of an “H2BTL” mutant array sample stained with SYBR® Gold. c) Depicts a Confocal microscope image of a “H2BTL & H3TL” mutant array sample stained with SYBR® Gold.

DISCUSSION

Octamer Preparation

Fast Protein Liquid Chromatography of a "Wild-Type" array containing an octamer with non-mutant histones was expected to yield an FPLC graph with three distinct mAU peaks. UV detections and resulting mAU peaks were expected to appear around 45 mL, 60 to 70 mL, and at 84 mL[20]. The first peak, around 45 mL was expected to contain a collection of any aggregate formed during preparation of the octamer. The next peak, between 60 and 70 mL was expected to contain the desired octamer. As tailless histone mutants are incorporated into these octamers, it was predicted that mAU peaks would be recorded slightly later on the FPLC graph. The last peak, at roughly 84 mL was thought to contain any excess H2A-H2B dimer that formed throughout the octamer preparation[19].

All Tailless

The All Tailless mutant FPLC graph contained three significant peaks. The first peak, corresponding to the aggregate was at roughly 42 mL. The second peak, corresponding to the octamer was at roughly 69 mL. The last peak, corresponding to the H2A-H2B dimer was at roughly 81 mL. The aggregate, octamer, and dimer peaks for the All Tailless mutant octamer registered UV readings at a at later volume within the column compared to the corresponding peaks of the H2BTL and H2BTL & H3TL mutant octamers. This was expected due to the significant decrease in molecular weight as more histone tails are excluded from the octamer[19]. Interestingly, this octamer mutant yielded the lowest concentration. An All Tailless octamer mutant with the lowest concentration compared to mutants with more tails could suggest a decreased ability or favorability with folding. This suggests that the presence of histone tails must be necessary for both octamer formation and chromatin condensate formation[18].

H2BTL

The H2BTL mutant FPLC graph also contained three significant peaks. All three peaks had a higher mAU value for the UV reading compared the corresponding peaks in the "All Tailless" and H2BTL & H3TL mutant octamers. The first peak, corresponding to the aggregate was at roughly 40 mL. The second peak, corresponding to the octamer was at roughly 61 mL. The third peak, corresponding to the dimer was at roughly 78 mL. The aggregate peak for this mutant had a relatively high mAU value compared to the aggregate peaks in the All Tailless and H2BTL & H3TL mutant octamers. The increase in mAU for the aggregate likely derived from the inaccurate addition of a 10-fold increase of the H2BTL mutant histone prior to dialysis[19]. This 10-fold increase of one histone could also account for the slight increase in mAU for the dimer associated peak, and for the additional mAU peak registered around115 mL. The additional mAU reading for this mutant was thought to be excess monomer. Compared to the All Tailless and H2BTL & H3TL mutants, refolding of the H2BTL octamer mutant yielded the highest octamer concentration. Having a higher octamer concentration could suggest an increased favorability of folding compared to octamer mutants with less histone tails.

H2BTL & H3TL

The H2BTL & H3TL mutant FPLC graph contained three significant peaks. The first peak, corresponding to the aggregate was at roughly 43 mL. This was recorded on the graph slightly later than the aggregate peaks for the All Tailless and H2BTL mutants. The second peak, corresponding to the octamer was at roughly 64 mL. The octamer peak for this mutant was detected with UV later than the H2BTL mutant, but not before the corresponding peak for the All tailless mutant octamer. This further suggested that UV readings for tailless mutant would appear shifted on the FPLC graphs based on the molecular weight of the octamer mutant. The

last peak, corresponding to the dimer was at roughly 80 mL. This dimer peak was also recorded on the graph earlier than the corresponding dimer for the H2BTL mutant, but not later than mAU dimer peak for the All Tailless mutant. The refolding process for this mutant yielded a concentration between the resulting H2BTL and All Tailless mutant. This further aided to the assumption that octamer concentration could be dependent on the favorability of binding for an octamer mutant.

601-12 Insert Preparation

The 601-12 tandem repeat DNA insert was expected to be roughly 2,496 base pairs in length. The final concentration of this insert was also expected to be above 1.00 mg/mL. Using a 1% agarose gel, a distinct band was visualized corresponding to about 2,500 base pairs in length. The concentration of the final resuspended 601-12 insert was also found to be about 1.3705 mg/mL. Reconstitution of the 601-12 insert and each octamer mutant was expected to yield 11 to 12 octamer mutants saturated along the insert[17]. Calculations were completed for each octamer mutant to confirm that a concentration of 1.3705 mg/mL could be used for reconstitution and that each repeat of 208 base pairs along the insert would be saturated with one octamer mutant.

601-12 Insert and Octamer Reconstitution

Appropriate volumes of the octamer variant, 601-12 insert and buffer 4 were then combined and dialyzed in buffers with decreasing NaCl concentrations. The success of each reconstituted mutant array was tested following dialysis. To determine the level of octamer saturation, the reconstituted mutant arrays were then tested via analytical ultracentrifugation and restriction enzyme digestion. The mutant arrays were then adjusted with the addition of insert or mutant octamers and redialyzed until a desired level of saturation was achieved. A desired level of saturation would suggest that each tandem repeat of about 208 base pairs in the 601 sequence

would have a single octamer associated. Therefore, along the 601-12 tandem repeat sequence, there should be roughly 12 octamers associated [17,21].

Analytical Ultracentrifugation

Analytical Ultracentrifugation (AUC) of a "Wild-type" non-mutant array containing a 601-12 tandem repeat sequence of DNA and roughly 11 to 12 octamers was expected to yield a sedimentation coefficient (S-value) of 29 S at a boundary fraction of 50[5,6]. It was also expected that as core histone tailless mutants are added, the S-value would decrease by a value of 1 S[5,6,16]. sedimentation coefficients resulting from analytical ultracentrifugation are dependent on size, molecular weights, extinction coefficients, rate of association, oxidation state, temperature, density, volume, and concentration[5,6].

All Tailless

The All Tailless mutant array consisted of the 601-12 tandem repeat sequence and an octamer containing all four tailless mutants of the core histones. According to these assumptions, it was predicted that AUC of an All Tailless mutant array should reflect a S-value close to 24S on a G(s) distribution[5,6,16]. When run through an ultracentrifuge, the All Tailless mutant array yielded the predicted value with an S-value just above 24 S. Molecular weight and size of the All tailless mutant as also decreased compared to a "Wild-type" or other array mutants[5,6]. Therefore, when comparing the S-value for this mutant array, it was expected that this mutant would have a decreased sedimentation coefficient compared to the H2BTL and H2BTL & H3TL mutant arrays. Based on obtaining an S-value of 24 for this mutant array, it was assumed that the 601 tandem DNA sequence for the All Tailless mutant array had been effectively saturated and that 11 – 12 mutant octamers were incorporated along the 601-12 insert. This was further confirmed using an EcoRI and EcoRV digestion.

H2BTL

The H2BTL mutant array contained an H2B tailless histone mutant. AUC results for this mutant array should reflect a an S-value close to 28 S. Out of all mutants tested, the H2BTL mutant should have the highest S-value as a result of the increased molecular weight compared to the other two mutants. Spinning this array through the ultracentrifuge yielded the expected value just above 28 S. Based on this value, it was assumed that the 601-12 tandem DNA sequence had the desired amount of H2BTL octamer mutant incorporated.

H2BTL & H3TL

The H2BTL & H3TL array contained an octamer mutant missing the H2B and H3 histone tails. It was expected that the S-value resulting from AUC would be around 27 S. Prior to re-dialysis of this array sample, there was a population around 37 S and a potential smaller population around 49 S. It was assumed based on these S-values that this sample was oversaturated with histone octamer mutants and that a second population could exist[5,6,16]. The significant increase in S-value reflects the presence of an increase in size and molecular weight for the H2BTL & H3TL mutant array. These resulting populations were also thought to result from the formation of higher order chromatin condensates in at least two different populations. Oversaturation of octamer mutants would likely result in G(s) distribution curves similar to the All Tailless and H2BTL mutant arrays. However, the resulting singular S-value would be much higher than expected[5,6]. Two potential S-values along the G(s) distribution more likely favors the presence of at least two populations of this mutant array. Octamer to DNA ratios were re-adjusted and more 601-12 insert was added to the mutant array sample before redialysis. Based on these calculations, it was assumed that the re-dialyzed sample would be closer to the expected S-values. The saturation level was then tested with an EcoRI and an EcoRV digestion.

EcoRI/EcoRV Digestion

All Tailless

Following determination of sedimentation coefficients with AUC, EcoRI and EcoRV digestions were performed to further verify saturation levels of each array sample. It was expected that lanes containing digested All Tailless mutant arrays and 25% glycerol/EDTA would reflect a smeared pattern ending slightly lower in base pairs than those of the lanes containing digested All Tailless mutant array and 6x-loading dye. The lanes containing digested mutant array and loading dye were also expected to have little to no presence of a distinct band aligned with the bottom of the lanes containing 25% glycerol/EDTA and digested array. The presence of a distinct band at the bottom of the loading dye and digested array sample lanes would suggest that "free DNA" still existed in solution and that the arrays were undersaturated[17]. With a sedimentation coefficient of 24 S and no presence of the distinct band at the bottom of the agarose gel, it was assumed that the 601-12 insert had reached a desired level of saturation with the All Tailless mutant octamer.

H2BTL

The lanes containing digested H2BTL mutant array and 25% glycerol/EDTA reflected similar results to the All Tailless mutant array. The lanes contained a smearing pattern that extended further than those in the lanes containing digested mutant array and loading dye. Lanes containing digested H2BTL array and 6x-loading dye were hardly visible on the agarose gel, however, no free DNA band was detected. With a sedimentation coefficient of 28 S and the absence of a distinct band at the bottom of these lanes, it was assumed that the 601-12 insert had been efficiently saturated with the H2BTL mutant octamer.

H2BTL & H3TL

The H2BTL & H3TL mutant array digestions were run on the same gel as the H2BTL mutant array. The lanes containing mutant array and 25% glycerol/EDTA were clearly visible and contained the expected smeared appearance along the gel. Lanes containing the H2BTL & H3TL mutant array and 6x-loading dye were difficult to visualize, but no free DNA band was detected. Due to the absence of this band thought to be free DNA, and a sedimentation coefficient above the expected S-value, it was assumed that the DNA insert had been at a minimum, fully saturated with this mutant octamer. Due to the high sedimentation coefficients resulting from AUC, oversaturation and the presence of multiple array populations was also considered.

Magnesium 50 Curves

All Tailless

Absorbance values for this mutant array did not reach a value 50% below the highest absorbance value and did not reach an absorbance value around zero. In all trials of the Magnesium 50 curves for the All Tailless mutant array, the absorbance (A_{260}) largely remained around a normalized value of 0.9 and was not dependent on increasing concentrations of $MgCl_2$. These consistent A_{260} values suggests that arrays containing an All Tailless mutant octamer cannot further associate into more complex chromatin condensate structures[8]. No further association or accessibility information could be determined for this mutant array. Therefore, Micrococcal Nuclease digestions and fluorescence microscopy experiments were not performed for this mutant array. Inability for the All Tailless mutant array to self-associate would suggest that at least one or more histone tails are necessary for a nucleosomal array to form higher order chromatin condensate structures[18].

H2BTL

H2BTL mutant arrays expressed a higher level of association compared to the All Tailless mutant arrays. In each trial of the Magnesium 50 curves for this mutant array, the A_{260} values seemed to decrease from a normalized value of 0.9 to zero as the $MgCl_2$ concentration was increased within the solution. The H2BTL mutant array seemed to be 50% associated close to a solution of 5 mM $MgCl_2$. Following 50% association, the H2BTL arrays seemed to reach total association in a lower concentration of $MgCl_2$ compared to the All Tailless and H2BTL & H3TL mutant arrays. Full association, with an absorbance close to zero, occurred in solutions at or around 8 mM $MgCl_2$. Considering this level of association, along with the favorability of octamer folding, this further suggests that chromosome condensate stability and formation is dependent on the presence of histone tails. As histone tails are withheld from octamer mutants, the ability of self-association of an array mutant is decreased.

H2BTL & H3TL

In all three trials for the H2BTL & H3TL mutant array, the A_{260} values were higher than the absorbance values for the All Tailless and H2BTL mutant arrays. Normalized absorbance values for this mutant array in 0 mM MgCl2 were recorded at or above 0.44 and decreased as $MgCl_2$ concentrations increased. This decrease in absorbance occurred until 50% association around an $MgCl_2$ concentration of 6 to 7 mM. The ability of further association recorded a slight decrease after $MgCl_2$ concentrations of 5 mM and had not fully reached an absorbance of zero around 10 mM $MgCl_2$. A slight decrease in absorbance after 50% association also supports the possibility of oversaturation or of the presence of multiple chromatin condensate populations from earlier experiments. Oversaturation, or the presence of larger chromatin condensates would likely result

in decreased absorbance values as well as little changes in absorbance values after a certain level of association as these mutant arrays reached increased levels of stability.

Micrococcal Nuclease Digestion

Micrococcal Nuclease (MNase) digestions were performed on the H2BTL and H2BTL & H3TL mutant arrays to determine the accessibility and stability of the 601-12 tandem repeat sequence in the presence of octamer mutants. Roughly 147 base pairs of DNA was expected to be protected from Micrococcal Nuclease digestion, were as the linker DNA between each nucleosome was susceptible to digestion[3,4].

H2BTL

Immediately after adding the MNase enzyme to the H2BTL mutant array, some of the reaction buffer solution was removed and placed in an equal volume of 2x stop reaction buffer. A zero time point was then measured. As expected, no digestion activity was observed for this time point. The band distance along the agarose gel also corresponded with an undigested nucleosomal array[3,4]. After five minutes, digestion began along the mutant arrays. Digestion levels increased at sequential time points. This increase of digestion at sequential time points suggested that the 601-12 repeat sequence increased in accessibility as time progressed. After 15 minutes, the H2BTL array was not fully digested. It was assumed that further digestion would occur at later time points.

H2BTL & H3TL

Interestingly, the (MNase) digestions performed on the H2BTL & H3TL mutant arrays reflected similar results to the H2BTL mutant array. Immediately after adding the MNase enzyme to the H2BTL & H3TL mutant array, the zero time point expressed little to no levels of digestion activity and the band distance was consistent with what was expected for the nucleosomal

arrays[3,4]. After five minutes, the arrays had similar levels of digestion compared to the H2BTL mutant array. After 15 minutes, the H2BTL & H3TL mutant array was also not fully digested. It was similarly assumed that the digestion would have been completed after a later time point. Comparing both MNase experiments for the H2BTL and H2BTL & H3TL mutants, no changes in accessibility were detected.

Fluorescence Microscopy

$MgCl_2$ solutions of each of the mutant and non-mutant array were standardized to 20 mM to ensure complete association[8,26]. A "Wild-type" nucleosomal array containing the high affinity 601 tandem repeat sequence and an non-mutated octamer was also imaged using fluorescence microscopy in order to provide an effective control and comparison between array mutants. The Wild-type array expressed an average chromatin condensate diameter of 0.216 μm. Between 600 to 700 condensates were visualized on each of the five "Wild-type" images. Both the H2BTL and the H2BTL & H3TL mutant arrays had a significant decrease in the number of condensates formed compared to the "Wild-type" array. As histone tails were withheld from the arrays, chromatin condensate diameters seemed to also increase.

H2BTL

The H2BTL chromatin condensate diameters had an average of about 0.334 μm and had about 340 to 430 condensates in each image. An octamer containing only one tailless mutant had little change in average condensate diameter, but had close to only half the number of condensates compared to the number visualized on the "Wild-type" images. A slight increase in condensate diameter could suggest a decreased ability for the chromatin condensates to fully associate into a "native" structure. However, visualizing a decrease in the number of overall condensates by half

proposes an idea that these chromatin condensate structures could be accumulating together and interacting.

H2BTL & H3TL

The average diameter for the H2BTL & H3TL mutant array was roughly 0.712, however, each image seemed to reflect the possibility of two or more populations. The presence of two populations within these images was further supported with the G(s) distributions given by the analytical ultracentrifuge and the Change in absorbances given by the Mg50 curves. Having H2B and H3 tailless mutants within an octamer had a drastic impact in increasing the average sizes of the condensate structures, likely resulting from the lack of coiled regions that normally pass through and directly interact with the DNA helix within the minor groove[18]. Two distinct populations within these arrays could suggest that H2B and H3 Tailless variants lead to loose compaction and decreased stability. Loose compaction could explain the increase in condensate diameter of one population. Loose compaction also supports the idea that the chromatin condensates may be accumulating and interacting with the neighboring condensates as regions within the arrays remained exposed. The accumulation of arrays into larger condensate structures could further explain the decrease in number of structures viewed in each of the mutant images compared to the "Wild-type" array. The images for the H2BTL & H3TL mutant contained only 150 to 210 globular structures.

Future Directions

G(s) distributions containing at least two populations for the H2BTL & H3TL mutant arrays deviated from the expected S-value of 27 S. In future experiments, reconstitution of the H2BTL & H3TL mutant octamer and 601-12 insert should be recalculated using an R value of 1.0 and the resulting mutant arrays should be reanalyzed with AUC and restriction enzyme digests.

Each of the previous experiments that had not been had multiple trials should be run through at least two additional times.

Tailless histone mutants for H3 and H2B seem to have a rather significant influence on the overall structure and stability within chromatin condensates. H2BTL mutant arrays seemed to have little difference from the "Wild-type" compared to the other two mutants. If an H4 and H2A tailless mutant was alternatively tested, it is seemingly unlikely that recombination, reconstitution, association, and condensate formation would express similar features. Similarly, testing an octamer containing three tailless histone mutants is necessary for comparison to previously tested mutants. Testing linker length and arrays with the addition of the linker histone H1 would also be beneficial.

It is also vital to compare these results with a non-mutant, or "Wild-type" octamer. "Wild-type" arrays were imaged along with two of the mutants tested, but were not used in comparison with the other experiments. Testing a "Wild-type" array with these methods would provide a crucial control for the previous experiments.

To Further confirm changes in structure, chromatin condensate stability, and exchange within these condensates, Fluorescence Recovery After Photobleaching (FRAP) analysis should also be performed.

CONCLUSION

The incorporation of specific tailless mutants in an octamer can lead to alterations in chromatin condensate structure, stability, and compaction. These alterations within the condensates can ultimately reflect similar changes *in vivo*. Deviations from "native" interactions within chromatin structure would lead to changes in accessibility to genetic material during various phases of the cell cycle. To better understand these changes, three octamer mutants (All Tailless, H2BTL, and H2BTL & H3TL) were tested *in vitro*. These mutants reconstituted with a 2,496 bp length of DNA and tested using a combination of experimental methods. Octamer saturation along the length of DNA was tested with analytical ultracentrifugation and confirmed with an EcoRI and EcoRV digestion. Each array was confirmed to be fully saturated with no remaining free DNA in solution. Magnesium 50 curves were then utilized to determine the ability and level of further association. As expected, The All Tailless octamer mutant expressed an inability to associate into more complex molecular structures, whereas the H2BTl and H2BTL & H3TL mutants further associated at appropriate magnesium concentrations. The accessibility of the H2BTL and H2BTL & H3TL mutant arrays was tested using fluorescence microscopy and supported with Micrococcal Nuclease digestions. A standardized concentration of 20 mM was used for the fluorescence microscopy experiments to ensure the arrays had fully associated and could form more complex structures. Compared to a "Wild-type" array, the H2BTL array mutant expressed a minor increase in size. The H2BTL & H3TL mutant had more notable increase in size and a possibility of two distinct condensate populations within solution. The exclusion of at least two tails suggests a more loosely compacted and easily accessible condensate structure compared to mutants excluding at least one histone tail. Taken together, this data suggests that as histone tails

are excluded from octamers, nucleosomal arrays express a decreased ability to form higher order structures and thus causes the 601-12 insert to be more accessible and susceptible to changes within chromatin condensate structures.

REFERENCES

1. Bilokapic, S., Strauss, M., & Halic, M. (2018). Structural rearrangements of the histone octamer translocate DNA. *Nature communications*, *9*(1), 1-11.

2. Blacketer, M. J., Feely, S. J., & Shogren-Knaak, M. A. (2010). Nucleosome interactions and stability in an ordered nucleosome array model system. *Journal of Biological Chemistry*, *285*(45), 34597-34607.

3. Chung, H. R., Dunkel, I., Heise, F., Linke, C., Krobitsch, S., Ehrenhofer-Murray, A. E., ... & Vingron, M. (2010). The effect of micrococcal nuclease digestion on nucleosome positioning data. *PloS one*, *5*(12).

4. Conolly, Mark., "Micrococcal Nuclease (MNase)." Protocol. Accessed March 11, 2020.

5. Demeler, B., Saber, H., & Hansen, J. C. (1997). Identification and interpretation of complexity in sedimentation velocity boundaries. *Biophysical journal*, *72*(1), 397.

6. Demeler, B. (2010). Methods for the design and analysis of sedimentation velocity and sedimentation equilibrium experiments with proteins. *Current protocols in protein science*, *60*(1), 7-13.

7. Dyer, P. N., Edayathumangalam, R. S., White, C. L., Bao, Y., Chakravarthy, S., Muthurajan, U. M., & Luger, K. (2003). Reconstitution of nucleosome core particles from recombinant histones and DNA. In *Methods in enzymology* (Vol. 375, pp. 23-44). Academic Press.

8. Hansen, J. C. (2002). Conformational dynamics of the chromatin fiber in solution: determinants, mechanisms, and functions. *Annual review of biophysics and biomolecular structure*, *31*(1), 361-392.

9. H2ATL, Scherman, M. A., Xenopus H2A Globular (a.a. 13-118) or Tailless. *The Histone Source (Protein Store)*. Accessed September 16, 2019. Retrieved from https://www.histonesource.com/protein-store#!/Xenopus-H2A-Globular-a-a-13-118-or-Tailless/p/59842171/category=16347606

10. H2BTL, Scherman, M. A., Xenopus H2B Globular (a.a. 24-122) or Tailless. *The Histone Source (Protein Store)*. Accessed September 16, 2019. Retrieved from https://www.histonesource.com/protein-store#!/Xenopus-H2B-Globular-a-a-24-122-or-Tailless/p/59842185/category=16347606

11. H3TL, Scherman, M. A., Xenopus H3TL Globular (a.a. 38-135) or Tailless. *The Histone Source (Protein Store)*. Accessed September 16, 2019. Retrieved from https://www.histonesource.com/protein-store#!/Xenopus-H3-Globular-a-a-38-135-or-Tailless-38-135/p/59842210/category=16347606

12. H4TL, Scherman, M. A., Xenopus H4TL Globular (a.a. 20-102) or Tailless. *The Histone Source (Protein Store)*. Accessed September 16, 2019. Retrieved from https://www.histonesource.com/protein-store#!/XenopusH4-Globular-20-102-or-Tailless/p/59842214/category=16347606

13. H4, Scherman, M. A., Xenopus H4. *The Histone Source (Protein Store)*. from Accessed May 1, 2019. Retrieved from https://www.histonesource.com/protein-store#!/Xenopus-H4/p/59842212/category=16347606

14. H3, Scherman, M. A., Xenopus H3. *The Histone Source (Protein Store)*. Accessed September 16, 2019. Accessed October 18, 2018. Retrieved from https://www.histonesource.com/protein-store#!/Xenopus-H3/p/59842186/category=16347606

15. H2A, Scherman, M. A., Xenopus H2A. *The Histone Source (Protein Store)*. Accessed May 1, 2019. Retrieved from https://www.histonesource.com/protein-store#!/Xenopus-H2A/p/59842170/category=16347606

16. Jamaluddin, M., & Philip, M. (1982). Histone octamer: dissociation in ultracentrifugal fields and subsequent reassociation into lower oligomers. *FEBS letters*, *150*(2), 429-433.

17. Lowary, P. T., & Widom, J. (1998). New DNA sequence rules for high affinity binding to histone octamer and sequence-directed nucleosome positioning. *Journal of molecular biology*, *276*(1), 19-42.

18. Luger, K., Mäder, A. W., Richmond, R. K., Sargent, D. F., & Richmond, T. J. (1997). Crystal structure of the nucleosome core particle at 2.8 Å resolution. *Nature*, *389*(6648), 251-260.

19. Luger, K., Rechsteiner, T. J., & Richmond, T. J. (1999). Preparation of nucleosome core particle from recombinant histones. In *Methods in enzymology* (Vol. 304, pp. 3-19). Academic Press.

20. Luger, K., "Histone Octamer Refolding." Protocol. Accessed September 19, 2019.

21. Maeshima, K., Rogge, R., Tamura, S., Joti, Y., Hikima, T., Szerlong, H., ... & Ishikawa, T. (2016). Nucleosomal arrays self-assemble into supramolecular globular structures lacking 30-nm fibers. *The EMBO journal*, *35*(10), 1115-1132.

22. Rogge, R. A., Kalashnikova, A. A., Muthurajan, U. M., Porter-Goff, M. E., Luger, K., & Hansen, J. C. (2013). Assembly of nucleosomal arrays from recombinant core histones and nucleosome positioning DNA. *JoVE (Journal of Visualized Experiments)*, (79), e50354.

23. Schwarz, P. M., & Hansen, J. C. (1994). Formation and stability of higher order chromatin structures. Contributions of the histone octamer. *Journal of Biological Chemistry*, *269*(23), 16284-16289.

24. Shaw, Allison. Fluorescence Microscopy Training. CNS-BMB-Confocal, Fort Collins, May 21, 2019.

25. Tolsma, Tommy. Fluorescence Microscopy and FRAP Imaging. CNS-BMB-Confocal, Fort Collins, March 20, 2020.

26. Tolsma, Tommy., "Microscopy Sample Preparation." Protocol. Accessed March 20, 2020.

27. Tolsma, Tommy., Kuerzi, Amanda., "Comprehensive 601-12 Bacterial Growth and Purification from Glycerol Stock." Protocol. Accessed October 26, 2019.

28. Tolsma, Tommy., "Mg 50 Curves." Protocol Accessed March 11, 2020.

29. Wilhelm, F. X., Wilhelm, M. L., Erard, M., & Daune, M. P. (1978). Reconstitution of chromatin: assembly of the nucleosome. *Nucleic acids research*, *5*(2), 505-521.

30. Yang, Z., & Hayes, J. J. (2011). The divalent cations Ca2+ and Mg2+ play specific roles in stabilizing histone–DNA interactions within nucleosomes that are partially redundant with the core histone tail domains. *Biochemistry*, *50*(46), 9973-9981.